DESY 14–199 ISSN 0418-9833
October 2014

Open charm production in the parton Reggeization approach: from Tevatron to LHC

M.A. Nefedov* and A.V. Karpishkov†

Samara State University, Ac. Pavlov, 1, 443011 Samara, Russia

V.A. Saleev‡

Samara State University, Ac. Pavlov, 1, 443011 Samara, Russia and
Samara State Aerospace University,
Moscow Highway, 34, 443086, Samara, Russia

A.V. Shipilova§

Samara State University, Ac. Pavlov, 1, 443011 Samara, Russia and
II. Institut für Theoretische Physik, Universität Hamburg,
Luruper Chaussee 149, 22761 Hamburg, Germany

Abstract

We study the inclusive hadroproduction of D^0, D^+, $D^{\star+}$, and D_s^+ mesons at leading order in the parton Reggeization approach endowed with universal fragmentation functions fitted to e^+e^- annihilation data from CERN LEP1. We have described D-meson transverse momentum distributions measured in the central region of rapidity by the CDF Collaboration at Tevatron ($|y| < 1$) and ALICE Collaboration at LHC ($|y| < 0.5$) within uncertainties and without free parameters, using Kimber-Martin-Ryskin unintegrated gluon distribution function in a proton. The forward D-meson production ($|y| > 2.0$) measured by the LHCb Collaboration also has been studied and expected disagreement between our theoretical predictions and data has been obtained.

PACS numbers: 12.38.-t,12.40.Nn,13.85.Ni,14.40.Gx

*Electronic address: nefedovma@gmail.com

†Electronic address: karpishkov@rambler.ru

‡Electronic address: saleev@samsu.ru

§Electronic address: alexshipilova@samsu.ru

I. INTRODUCTION

The study of the open charm production in the high energy hadronic collisions is considered as a test of general applicability of perturbative quantum chromodynamics (QCD). In the process of charmed meson production one has $\mu \geq m$, where μ is the typical energy scale of the hard interaction, m is the charm quark mass, and $\alpha_S(\mu) \ll 1$. Nevertheless, this study is also our potential for the observation of a new dynamical regime of perturbative QCD, namely the high-energy *Regge limit*, which is characterized by the following condition $\sqrt{S} \gg \mu \gg \Lambda_{QCD}$, where $\sqrt{S}$ is the invariant collision energy, and Λ_{QCD} is the asymptotic scale parameter of QCD. In this limit a new small parameter $x \sim \mu/\sqrt{S}$ appears.

The small-x effects cause the distinction of the perturbative corrections relative for different processes and different regions of phase space. At first, the higher-order corrections for the production of heavy final states, such as Higgs bosons, top-quark pairs, dijets with large invariant masses, or Drell-Yan pairs, by initial-state partons with relatively large momentum fractions $x \sim 0.1$ are dominated by soft and collinear gluons and may increase the cross sections up to a factor 2. By contrast, relatively light final states, such as small-transverse-momentum heavy quarkonia, single jets, prompt photons, or dijets with small invariant masses, are produced by the fusion of partons with small values of x, typically $x \sim 10^{-3}$ because of the large values of $\sqrt{S}$. Radiative corrections to such processes are dominated by the production of additional hard jets. The only way to treat such processes in the conventional collinear parton model (CPM) is to calculate higher-order corrections in the strong coupling constant $\alpha_S = g_S^2/4\pi$, which could be a challenging task for some processes even at the next-to-leading order (NLO) level. To overcome this difficulty and take into account a sizable part of the higher-order corrections in the small-x regime, the k_T-factorization framework, was introduced [1–3].

Recently the ALICE Collaboration measured the differential cross sections $d\sigma/dp_T$ for the inclusive production of D^0, D^+, $D^{\star+}$, and D_s^+ mesons [4–6] in proton-proton collisions at the CERN LHC ($\sqrt{S} = 2.76; 7$ TeV) as functions of D-meson transverse momentum (p_T) in the central rapidity region, $|y| < 0.5$. These measurements extend the CDF Collaboration data [7] obtained earlier in proton-antiproton collisions at the Fermilab Tevatron at the $|y| < 1.0$ and $\sqrt{S} = 1.96$ TeV. The production of D-mesons in the forward rapidity region of $2.0 < y < 4.5$ was investigated at the LHC by LHCb Collaboration and the data in the

form of $d\sigma/dp_T$ were presented for the different intervals of rapidity [8].

These data have been studied in the next-to-leading order (NLO) in the collinear parton model of QCD within the two approaches: the general-mass variable-flavor-number (GM-VFN) scheme [9], and the so-called fixed order scheme improved with next-to-leading logarithms (FONLL scheme) [10]. In the former one, realized in the Refs. [11–13], the large fragmentation logarithms dominating at $p_T >> m$ are resummed through the evolution of the fragmentation functions (FFs), satisfying the Dokshitzer-Gribov-Lipatov-Altarelli-Parisi (DGLAP) [14] evolution equations. At the same time, the full dependence on the charm-quark mass in the hard-scattering cross section is retained to describe consistently $p_T \sim m$ region. The D-meson FFs were extracted both at leading and next-to-leading order in the GM-VFN scheme from the fit of e^+e^- data taken by the OPAL Collaboration at CERN LEP1 [15]. Opposite, in the FONLL approach, the NLO D-meson production cross sections are calculated with a non-perturbative c-quark FF, that is not a subject to DGLAP [14] evolution. The FONLL scheme was implemented in the Refs. [16, 17] and its main ingredients are the following: the NLO fixed order calculation (FO) with resummation of large transverse momentum logarithms at the next-to-leading level (NLL) for heavy quark production. For the consistency of the calculation, the NLL formalism should be used to extract the nonperturbative FFs from e^+e^- data, and in the Refs. [16, 17] the scheme of calculation of heavy quark cross section and extraction of the nonperturbative FFs are directly connected and must be used only together.

The overall agreement of data and calculations obtained in Refs. [11–13, 16, 17] is good, the $D-$meson spectra measured by the CDF Collaboration at the Fermilab Tevatron and ALICE and LHCb Collaborations at the LHC are described within experimental uncertainties.

The aim of the present work is to study the D-meson production at Fermilab Tevatron and CERN LHC in the framework of high-energy factorization scheme, namely k_T-factorization framework [1] endowed with the fully gauge-invariant amplitudes with *Reggeized* gluons in the initial state. This combination we will call the Parton Reggeization Approach (PRA) everywhere below.

The study of D-meson fragmentation production in terms of k_T-factorization [1–3] was performed also previously in the recent work [18], with off-shell initial gluons and using the formalism of transverse-momentum dependent parton distributions, whereas the first

results in this scheme were obtained for the D_0 production at Tevatron Run I [19]. The resulting curve in Ref. [18] describes the ALICE experimental data [5] by its upper limit of theoretical uncertainty. We suppose PRA to be more theoretically consistent than previous studies in k_T-factorization, being not a recipe but based on a gauge invariant effective theory for the processes in quasi-multi-Regge kinematics (QMRK) in QCD. Therefore it preserves the gauge invariance of high-energy particle production amplitudes and allows a consistent continuation towards the NLO calculations.

Recently, PRA was successfully applied for the analysis of inclusive production of single jet [20], pair of jets [21], prompt-photon [22, 23], photon plus jet [24], Drell-Yan lepton pairs [25], bottom-flavored jets [26, 27], charmonium and bottomonium production [28–32] at the Tevatron and LHC. These studies have demonstrated the advantages of the high-energy factorization scheme based on PRA in the descriptions of data comparing to the collinear parton model calculations.

This paper is organized as follows. In Sec. II we present basic formalism of our calculations, the PRA and the fragmentation model. In Sec. III our results are presented in comparison with the experimental data and discussed. In Sec. IV we summarize our conclusions.

II. BASIC FORMALISM

The phenomenology of strong interactions at high energies exhibits a dominant role of gluon fusion into heavy quark and antiquark pair in heavy meson production. As it was shown in Ref. [11], a significant part of D-meson production cross section comes from gluon and c-quark fragmentation into D-meson, and the light quark fragmentation turns out to be negligible. Following this, in our study we will consider the c-quark and gluon fragmentation into different D-mesons only.

In hadron collisions the cross sections of processes with a hard scale μ can be represented as a convolution of scale-dependent parton (quark or gluon) distributions and squared hard parton scattering amplitude. These distributions correspond to the density of partons in the proton with longitudinal momentum fraction x integrated over transverse momentum up to $k_T = \mu$. Their evolution from some scale μ_0, which controls a non-perturbative regime, to the typical scale μ is described by DGLAP [14] evolution equations which allow to sum

large logarithms of type $\log(\mu^2/\Lambda^2_{QCD})$ (collinear logarithms). The typical scale μ of the hard-scattering processes is usually of order of the transverse mass $m_T = \sqrt{m^2 + |\mathbf{p}_T|^2}$ of the produced particle (or hadron jet) with (invariant) mass m and transverse two-momentum $\mathbf{p}_T$. With increasing energy, when the ratio of $x \sim \mu/\sqrt{S}$ becomes small, the new large logarithms $\log(1/x)$, soft logarithms, are to appear and can become even more important than the collinear ones. These logarithms present both in parton distributions and in partonic cross sections and can be resummed by the Balitsky-Fadin-Kuraev-Lipatov (BFKL) approach [33]. The approach gives the description of QCD scattering amplitudes in the region of large S and fixed momentum transfer t, $S \gg |t|$ (Regge region), with various color states in the t-channel. Entering this region requires us to reduce approximations to keep the true kinematics of the process. It becomes possible introducing the unintegrated over transverse momenta parton distribution functions (UPDFs) $\Phi(x, t, \mu^2)$, which depend on parton transverse momentum $\mathbf{q}_T$ while its virtuality is $t = -|\mathbf{q}_T|^2$. The UPDFs are defined to be related with collinear ones through the equation:

$$xG(x, \mu^2) = \int^{\mu^2} dt \Phi(x, t, \mu^2). \tag{1}$$

The UPDFs satisfy the BFKL evolution equation [33] which is suited to resum soft logarithms and appear in the BFKL approach as a particular result in the study of analytical properties of the forward scattering amplitude. The basis of the BFKL approach is the gluon Reggeization [34], as at small x the gluons are the dominant partons.

The gluon Reggeization appears considering special types of kinematics of processes at high-energies. At large $\sqrt{S}$ the dominant contributions to cross sections of QCD processes gives multi-Regge kinematics (MRK). MRK is the kinematics where all particles have limited (not growing with $\sqrt{S}$) transverse momenta and are combined into jets with limited invariant mass of each jet and large (growing with $\sqrt{S}$) invariant masses of any pair of the jets. At leading logarithmic approximation of the BFKL approach (LLA), where the logarithms of type $(\alpha_s \log(1/x))^n$ are resummed, only gluons can be produced and each jet is actually a gluon. At next-to-leading logarithmic approximation (NLA) the terms of $\alpha_s(\alpha_s \log(1/x))^n$ are collected and a jet can contain a couple of partons (two gluons or quark-antiquark pair). Such kinematics is called quasi multi-Regge kinematics. Despite of a great number of contributing Feynman diagrams it turns out that at the Born level in the MRK amplitudes acquire a simple factorized form. Moreover, radiative corrections to these amplitudes do

not destroy this form, and their energy dependence is given by Regge factors $s_i^{\omega(q_i)}$, where s_i are invariant masses of couples of neighboring jets and $\omega(q_i)$ can be interpreted as a shift of gluon spin from unity, dependent from momentum transfer q. This phenomenon is called gluon Reggeization.

Due to the Reggeization of quarks and gluons, an important role is dedicated to the vertices of Reggeon-particle interactions. In particular, these vertices are necessary for the determination of the BFKL kernel. To define them we can notice the two ways: the "classical" BFKL method [35] is based on analyticity and unitarity of particle production amplitudes and the properties of the integrals corresponding to the Feynman diagrams with two particles in the t-channel has been developed. Alternatively, they can be straightforwardly derived from the non-Abelian gauge-invariant effective action for the interactions of the Reggeized partons with the usual QCD partons, which was firstly introduced in Ref. [36] for Reggeized gluons only, and then extended by inclusion of Reggeized quark fields in the Ref. [37]. The full set of the induced and effective vertices together with Feynman rules one can find in Refs. [37, 38].

Recently, an alternative method to obtain the gauge-invariant $2 \to n$ amplitudes with off-shell initial-state partons, which is mathematically equivalent to the PRA, was proposed in Ref. [39]. These $2 \to n$ amplitudes are extracted by using the spinor-helicity representation with complex momenta from the auxiliary $2 \to n+2$ scattering processes which are constructed to include the $2 \to n$ scattering processes under consideration. This method is more suitable for the implementation in automatic matrix-element generators, but for our study the use of Reggeized quarks and gluons is found to be simpler.

As we mentioned above, we will consider the D-meson production by only the c-quark and gluon fragmentation. The lowest order in α_S parton subprocesses of PRA in which gluon or c-quark are produced are the following: a gluon production via two Reggeized gluon fusion

$$\mathcal{R} + \mathcal{R} \to g, \tag{2}$$

and the corresponding quark-antiquark pair production

$$\mathcal{R} + \mathcal{R} \to c + \bar{c}, \tag{3}$$

where $\mathcal{R}$ are the Reggeized gluons.

According to the prescription of Ref. [38], the amplitudes of relevant processes (2) and (3) can be obtained from the Feynman diagrams depicted in Figs. 1 and 2, where the dashed

lines represent the Reggeized gluons. Of course, the last three Feynman diagrams in Fig. 2 can be combined into the effective particle-Reggeon-Reggeon (PRR) vertex [38].

Let us define four-vectors $(n^-)^\mu = P_1^\mu/E_1$ and $(n^+)^\mu = P_2^\mu/E_2$, where $P_{1,2}^\mu$ are the four-momenta of the colliding protons, and $E_{1,2}$ are their energies. We have $(n^\pm)^2 = 0$, $n^+ \cdot n^- = 2$, and $S = (P_1 + P_2)^2 = 4E_1E_2$. For any four-momentum k^μ, we define $k^\pm = k \cdot n^\pm$. The four-momenta of the Reggeized gluons can be represented as

$$\begin{aligned} q_1^\mu &= \frac{q_1^+}{2}(n^-)^\mu + q_{1T}^\mu, \\ q_2^\mu &= \frac{q_2^-}{2}(n^+)^\mu + q_{2T}^\mu, \end{aligned} \tag{4}$$

where $q_T = (0, \mathbf{q}_T, 0)$ The amplitude of gluon production in fusion of two Reggeized gluons can be presented as scalar product of Fadin-Kuraev-Lipatov effective PRR vertex $C_{\mathcal{R}\mathcal{R}}^{g,\mu}(q_1, q_2)$ and polarization four-vector of final gluon $\varepsilon_\mu(p)$:

$$\mathcal{M}(\mathcal{R} + \mathcal{R} \to g) = C_{\mathcal{R}\mathcal{R}}^{g,\mu}(q_1, q_2)\varepsilon_\mu(p), \tag{5}$$

where

$$\begin{aligned} C_{\mathcal{R}\mathcal{R}}^{g,\mu}(q_1, q_2) \;=\; & -\sqrt{4\pi\alpha_s} f^{abc} \frac{q_1^+ q_2^-}{2\sqrt{t_1 t_2}} \left[(q_1 - q_2)^\mu + \frac{(n^+)^\mu}{q_1^+} \left(q_2^2 + q_1^+ q_2^- \right) \right. \\ & \left. - \; \frac{(n^-)^\mu}{q_2^-} \left(q_1^2 + q_1^+ q_2^- \right) \right], \end{aligned} \tag{6}$$

a and b are the color indices of the Reggeized gluons with incoming four-momenta q_1 and q_2, and f^{abc} with $a = 1, ..., N_c^2 - 1$ is the antisymmetric structure constants of color gauge group $SU_C(3)$. The squared amplitude of the partonic subprocess $\mathcal{R} + \mathcal{R} \to g$ is straightforwardly found from Eq. (6) to be

$$\overline{|\mathcal{M}(\mathcal{R} + \mathcal{R} \to g)|^2} = \frac{3}{2}\pi\alpha_s \mathbf{p}_T^2. \tag{7}$$

The amplitude of the process (3) can be presented in a same way, as a sum of three terms $\mathcal{M}(\mathcal{R} + \mathcal{R} \to c + \bar{c}) = \mathcal{M}_1 + \mathcal{M}_2 + \mathcal{M}_3$:

$$\begin{aligned} \mathcal{M}_1 &= -i\pi\alpha_s \frac{q_1^+ q_2^-}{\sqrt{t_1 t_2}} T^a T^b \bar{U}(p_1)\gamma^\alpha \frac{\hat{p}_1 - \hat{q}_1}{(p_1 - q_1)^2}\gamma^\beta V(p_2)(n^+)^\alpha (n^-)^\beta, \\ \mathcal{M}_2 &= -i\pi\alpha_s \frac{q_1^+ q_2^-}{\sqrt{t_1 t_2}} T^b T^a \bar{U}(p_1)\gamma^\beta \frac{\hat{p}_1 - \hat{q}_2}{(p_1 - q_2)^2}\gamma^\alpha V(p_2)(n^+)^\alpha (n^-)^\beta, \\ \mathcal{M}_3 &= 2\pi\alpha_s \frac{q_1^+ q_2^-}{\sqrt{t_1 t_2}} T^c f^{abc} \frac{\bar{U}(p_1)\gamma^\mu V(p_2)}{(p_1 + p_2)^2} [(n^-)^\mu (q_2^+ + \frac{q_2^2}{q_1^-}) - (n^+)^\mu (q_1^- + \frac{q_1^2}{q_2^+}) + (q_1 - q_2)^\mu], \end{aligned} \tag{8}$$

where T^a are the generators of the fundamental representation of the color gauge group $SU_C(3)$.

The squared amplitudes can be presented as follows

$$\overline{|\mathcal{M}(\mathcal{R}+\mathcal{R}\to c+\bar{c})|^2} = 256\pi^2\alpha_s^2\left(\frac{1}{2N_c}\mathcal{A}_{\rm Ab}+\frac{N_c}{2(N_c^2-1)}\mathcal{A}_{\rm NAb}\right) \tag{9}$$

$$\mathcal{A}_{\rm Ab} = \frac{t_1t_2}{\hat{t}\hat{u}} - \left(1+\frac{p_2^+}{\hat{u}}(q_1^- - p_2^-)+\frac{p_2^-}{\hat{t}}(q_2^+-p_2^+)\right)^2 \tag{10}$$

$$\begin{aligned}\mathcal{A}_{\rm NAb} \;=\; & \frac{2}{S^2}\left(\frac{p_2^+(q_1^- - p_2^-)S}{\hat{u}}+\frac{S}{2}+\frac{\Delta}{\hat{s}}\right)\left(\frac{p_2^-(q_2^+-p_2^+)S}{\hat{t}}+\frac{S}{2}-\frac{\Delta}{\hat{s}}\right)\\ & -\frac{t_1t_2}{q_1^-q_2^+\hat{s}}\left(\left(\frac{1}{\hat{t}}-\frac{1}{\hat{u}}\right)(q_1^-p_2^+ - q_2^+p_2^-)+\frac{q_1^-q_2^+\hat{s}}{\hat{t}\hat{u}}-2\right)\end{aligned} \tag{11}$$

$$\Delta = \frac{S}{2}\left(\hat{u}-\hat{t}+2q_1^-p_2^+-2q_2^+p_2^-+t_1\frac{q_2^+-2p_2^+}{q_2^+}-t_2\frac{q_1^--2p_2^-}{q_1^-}\right) \tag{12}$$

Here the bar indicates averaging (summation) over initial-state (final-state) spins and colors, $t_1=-q_1^2=|\mathbf{q}_{1T}|^2$, $t_2=-q_2^2=|\mathbf{q}_{2T}|^2$, and

$$\begin{aligned}\hat{s} &= (q_1+q_2)^2=(p_1+p_2)^2,\\ \hat{t} &= (q_1-p_1)^2=(q_2-p_2)^2,\\ \hat{u} &= (q_2-p_1)^2=(q_1-p_2)^2.\end{aligned}$$

The squared amplitude (9) analytically coincide with the previously obtained in Ref. [1]. We checked that in the collinear limit, i.e. $q_{(1,2)T}\to 0$, the squared amplitude (9) after averaging over the azimuthal angles transforms to the squared amplitude of the corresponding parton subprocess in collinear model, namely $g+g\to c+\bar{c}$. We perform our analysis in the region of $\sqrt{S}, p_T \gg m_c$, that allows us to use zero-mass variable-flavor-number-scheme (ZM VFNS), where the masses of the charm quarks in the hard-scattering amplitude are neglected.

In the k_T-factorization, differential cross section for the $2\to 1$ subprocess (2) has the form:

$$\frac{d\sigma}{dydp_T}(p+p\to g+X) = \frac{1}{p_T^3}\int d\phi_1\int dt_1\Phi(x_1,t_1,\mu^2)\Phi(x_2,t_2,\mu^2)\overline{|\mathcal{M}(\mathcal{R}+\mathcal{R}\to g)|^2}, \tag{13}$$

where ϕ_1 is the azimuthal angle between $\mathbf{p}_T$ and $\mathbf{q}_{1T}$.

Analogous formula for the $2 \to 2$ subprocess (3) can be written as

$$\frac{d\sigma}{dy_1 dy_2 dp_{1T} dp_{2T}}(p + p \to c(p_1) + \bar{c}(p_2) + X) = \frac{p_{1T} p_{2T}}{16\pi^3} \int d\phi_1 \int d\Delta\phi \int dt_1 \times$$
$$\times \Phi(x_1, t_1, \mu^2) \Phi(x_2, t_2, \mu^2) \frac{\overline{|\mathcal{M}(\mathcal{R} + \mathcal{R} \to c + \bar{c})|^2}}{(x_1 x_2 S)^2}, \qquad (14)$$

where $x_1 = q_1^+/P_1^+$, $x_2 = q_2^-/P_2^-$, $\Delta\phi$ is the azimuthal angle between $\mathbf{p}_{1T}$ and $\mathbf{p}_{2T}$, the rapidity of the final-state parton with four-momentum p is $y = \frac{1}{2}\ln(\frac{p^+}{p^-})$. Again, we have checked a fact that in the limit of $t_{1,2} \to 0$, we recover the conventional factorization formula of the collinear parton model from (13) and (14).

The important ingredient of the our scheme is unintegrated gluon distribution function, which we take as one proposed by Kimber, Martin and Ryskin (KMR) [40]. These distributions are obtained introducing a single-scale auxiliary function which satisfies the unified BFKL/DGLAP evolution equation, where the leading BFKL logarithms $\alpha_S \log(1/x)$ are fully resummed and even a major (kinematical) part of the subleading BFKL effects are taken into account. This procedure to obtain UPDFs requires less computational efforts than the precise solution of two-scale evolution equations such as, for instance, Ciafaloni-Catani-Fiorani-Marchesini equation [41], but we found it to be suitable and adequate to physics of processes under study.

The usage of the k_T-factorization formula and UPDFs with one longitudinal (light-cone) kinematic variable (x) requires the Reggeization of the $t-$channel partons. Accordingly to Refs. [36, 37], Reggeized partons carry only one large light-cone component of the four-momentum and, therefore, it's virtuality is dominated by the transverse momentum. Such kinematics of the $t-$channel partons corresponds to the MRK of the initial state radiation and particles, produced in the hard process. In our previous analysis [28–32] devoted to the similar processes of heavy meson production we proved that these UPDFs give the best description of the heavy quarkonium p_T-spectra measured at the Tevatron [42] and LHC [43].

In the fragmentation model the transition from the produced gluon or c-quark to the D-meson is described by fragmentation function $D_{c,g}(z, \mu^2)$. According to corresponding factorization theorem of QCD and the fragmentation model, the basic formula for the D-

meson production cross section reads [44]:

$$\frac{d\sigma(p+p\to D+X)}{dp_{DT}dy}=\sum_i\int_0^1\frac{dz}{z}D_{i\to D}(z,\mu^2)\frac{d\sigma(p+p\to i(p_i=p_D/z)+X)}{dp_{iT}dy_i}, \qquad (15)$$

where $D_{i\to D}(z,\mu^2)$ is the fragmentation function for the parton i, produced at the hard scale μ, splitting into D-meson, z is the longitudinal momentum fraction of a fragmenting particle carried by the D-meson. In the zero-mass approximation the fragmentation parameter z can be defined as follows $p_D^\mu=zp_i^\mu$, p_D and p_i are the $D-$meson and i-parton four-momenta, and $y_D=y_i$. In our calculations we use the LO FFs from Ref. [12], where the fits of non-perturbative D^0, D^+, $D^{\star+}$, and D_s^+ FF's, both at LO and NLO in the $\overline{\rm MS}$ factorization scheme, to OPAL data from LEP1 [15] were performed. These FFs satisfy two desirable properties: at first, their $\mu-$scaling violation is ruled by DGLAP evolution equations; at second, they are universal.

In the fits of Refs. [11–13], the parameterizations at the initial scale $\mu_0=m_c$ for the FF's were taken as follows:

$$D_c(z,\mu_0^2)=N_c\frac{z(1-z)^2}{[(1-z)+\epsilon_c]^2} \qquad (16)$$

$$D_{g,q}(z,\mu_0^2)=0. \qquad (17)$$

To illustrate a difference of contributions to the D-meson production we show in the Fig. 3 the $c-$quark and gluon FF's into $D^\star-$meson.

As the contribution of gluon fragmentation at $\mu>\mu_0$ is initiated by the perturbative transition of gluons to $c\bar{c}$-pairs encountered by DGLAP evolution equations, the part of c-quarks produced in the subprocess (3) with their subsequent transition to D-mesons are already taken into account considering D-meson production via gluon fragmentation. Such a way, to avoid double counting, we must subtract this contribution, that can be effectively done by the imposing of the lower cut on $\hat{s}$ at the threshold of the production of the $c\bar{c}$ pair in (14), i.e $\hat{s}>4m_c^2$. The precise study of double-counting terms and other finite-mass effects needs a separate consideration and can be a subject of our future works.

III. RESULTS

The first measurement of D-meson production transverse-momentum distributions at hadron colliders was implemented by the CDF Collaboration at Fermilab Tevatron [7], at

the collision energy of $\sqrt{S} = 1.96$ TeV. The production of the D^0, D^+, $D^{\star+}$, and D_s^+ mesons was studied in the central region of rapidity $|y| < 1.0$ and with transverse momenta up to 20 GeV. In the Fig. 4 we introduce these data coming as differential cross sections $d\sigma/dp_T$, where the particle and antiparticle contributions are averaged, in comparison with our predictions in the PRA. The dashed lines represent contributions of the process (2) while dash-dotted lines correspond to ones of the process (3). The sum of both contributions is shown as solid line. We estimated a theoretical uncertainty arising from uncertainty of definition of factorization and renormalization scales by varying them between $1/2m_T$ and $2m_T$ around their central value of m_T, the transverse mass of fragmenting parton. The resulting uncertainty is depicted in the figures by shaded bands. We find a good agreement between our predictions and experimental data in the large-p_T interval of D-meson transverse momenta within experimental an theoretical uncertainties. However, our predictions show a tendency to fall below the data in the lower p_T range. It can point to the significance of c-quark mass effects in the region, where the hard scale of the process is not much larger than the c-quark mass. The increasing of the collision energy with other kinematic conditions preserved is supposed to lead to a better agreement between theory and experiment in our approach as we expect the rise of logarithmic contributions of type $\log(1/x)$ to be more significant than finite-quark-mass effects.

Our expectations are confirmed when we turn to the description of the recent data from the LHC at its intermediate energy of $\sqrt{S} = 2.76$ TeV and $\sqrt{S} = 7$ TeV collected by the ALICE Collaboration [4, 5]. The previous NLO predictions made in collinear parton model in general are in agreement with ALICE data, however, one can find that the FONLL scheme [17] tend to overestimate data and the GM-VFN [13] is to underestimate. In the Figs. 5 and 6, we compare our predictions with ALICE data [4, 5] keeping the notations of curves the same as in the Fig. 4. The current collision energies of LHC is 2-3.5 times larger compared to Tevatron and the interval of D-meson rapidity is more narrow, $|y| < 0.5$. We obtain a good agreement of our predictions with the experiment for the all types of D-mesons at the whole range of their transverse momenta. As there is no experimental data for D_s^+-production at the energy of $\sqrt{S} = 2.76$ TeV, we introduce the theoretical prediction only. Finally, in the Fig. 7 we present our predictions for the planned LHC energy of $\sqrt{S} = 14$ TeV and the other kinematic conditions as in the Ref. [5].

Considering the D-meson central rapidity production, we find the MRK subprocess (2)

to remain indeed the dominant one for all collision energies. Such a way, we confirm the theoretical suggestion mentioned in Sec. II that MRK gives the leading logarithmic approximation for the high-energy production processes in BFKL approach while the QMRK turns out to be subleading. However, in the framework of Ref. [18], which seems to be theoretically close to PRA, this MRK subprocess is absent while the main contribution is coming from QMRK subprocess.

Not only the central but also the forward rapidity region in pp collisions at the LHC become available due to the specially designed LHCb detector where the measurements of differential cross sections of D^0, D^+, $D^{\star+}$, and D_s^+ mesons with $2.0 < y < 4.5$ at $\sqrt{S} = 7$ TeV were performed [8]. The observed data divided into 5 rapidity regions have been under study in both, FONLL and GM-VFN, schemes and were founded to be generally enclosed between their predictions [13, 17]. We present these data together with our results obtained in the LO of PRA in the Figs. 8-12. One can find the summary contribution mainly to underestimate the data from 1.5 to 2 times with a slight exception in the case of D_s^+ production. This result is expected and becomes clear if we recall that with grow of rapidity of the particle produced in the hard scattering process the fraction of longitudinal momenta of initial proton transferred to this process increases simultaneously. That means, on a one hand, that we enter the region of large $x > 0.1$ where the conditions of Reggeization are not satisfied, and another effects, such as signals of intrinsic charm, can appear. On the other hand, to balance the large positive rapidity of a produced particle one needs a very small negative longitudinal momenta to income the hard subprocess from the side of another proton in the collision. Such a way, we have a very asymmetric case where the one t-channel exchange is perfectly under the multi-Regge kinematics conditions being strong opposite the second one. That leads to the situation in which we finely take into account small-x effects although loosing in large-x. It is illustrated by the Fig. 12 dedicated to the largest rapidity region $4.0 < y < 4.5$ where we obtain a better agreement with experimental data in comparison with other ones of forward production. It proves our assumption that BFKL-type logarithms exhibit themselves at the already achieved collision energies giving a significant contribution to the production rates.

Considering the relative contributions of the subprocesses in the forward rapidity region, we find the QMRK subprocess to decrease with grow of rapidity. That illustrates the fact that the probability of a production of quark and antiquark both with large close rapidities

in a symmetric collision diminishes. The case when one of them has a significant positive rapidity, and another one – the same negative, contradicts the definition of QMRK process.

IV. CONCLUSIONS

We introduce a comprehensive study of D^0, D^+, $D^{\star+}$, and D_s^+-meson fragmentation production in proton-(anti)proton collisions with central rapidities at Tevatron Collider and LHC and in the forward rapidity region for the LHC, in the framework of Parton Reggeization Approach. We use the gauge invariant amplitudes of hard parton subprocesses in the LO level of theory with Reggeized gluons in the initial state in a self-consistent way together with unintegrated parton distribution functions proposed by Kimber, Martin and Ryskin. The $2 \to 1$ hard subprocess of gluon production via a fusion of two Reggeized gluons in the PRA framework is proposed for the first time in the case of D-meson fragmentation production and proved to be a dominant one. To describe the non-perturbative transition of produced gluons and c-quarks into the D-mesons we use the universal fragmentation functions obtained from the fit of e^+e^- annihilation data from CERN LEP1. We found our results for D-meson central-rapidity production to be in the excellent coincidence with experimental data from the LHC and good agreement with large-transverse-momenta Tevatron data. The achieved degree of agreement for the LHC exceeds the one obtained by NLO calculations in the conventional collinear parton model and LO calculations in k_T-factorization with Reggeized gluons. The predictions for the D-meson production in the central rapidity region for the expected LHC energy of $\sqrt{S} = 14$ TeV are also presented. For the forward rapidity region we compare our results with transverse-momentum D-meson distributions measured by LHCb Collaboration at LHC, and the expected discrepancies are obtained. We describe D-meson production without any free parameters or auxiliary approximations.

V. ACKNOWLEDGEMENTS

The work of A. V. Shipilova and A. V. Karpishkov was partly supported by the Grant of President of Russian Federation No. MK-4150.2014.2. The work of M.A. Nefedov and V.A. Saleev was supported in part by the Russian Foundation for Basic Research through the Grant No. 14-02-00021. A. V. Shipilova is grateful to Prof. G. Kramer for the useful

discussions, to Prof. B. A. Kniehl for the kind hospitality, and to the German Academic Exchange Service (DAAD) together with the Russian Federal Ministry of Science and Education for the financial support by Grant No. A/13/75500.

---

[1] J. C. Collins and R. K. Ellis, Nucl. Phys. **B360**, 3 (1991).

[2] L. V. Gribov, E. M. Levin, and M. G. Ryskin, Phys. Rep. **100**, 1 (1983).

[3] S. Catani, K. M. Ciafaloni, and F. Hautmann, Nucl. Phys. **B366**, 135 (1991).

[4] ALICE Collaboration, B. Abelev *et al.*, JHEP **1201**, 128 (2012).

[5] ALICE Collaboration, B. Abelev *et al.*, JHEP **1207**, 191 (2012).

[6] ALICE Collaboration, B. Abelev *et al.*, Phys. Lett. **B718**, 279 (2012).

[7] CDF Collaboration, D. Acosta *et al.*, Phys. Rev. Lett. **91**, 241804 (2003).

[8] LHCb Collaboration, R. Aaij *et al.*, Nucl.Phys. **B871**, 1-20 (2013).

[9] G. Kramer, and H. Spiesberger, Eur. Phys. J. C **22**, 289 (2001); **28**, 495 (2003); **38**, 309 (2004); B. A. Kniehl, G. Kramer, I. Schienbein, and H. Spiesberger, Phys. Rev. D **71**, 014018 (2005); B. A. Kniehl, G. Kramer, I. Schienbein, and H. Spiesberger, Eur. Phys. J. C **41**, 199 (2005).

[10] M. Cacciari, M. Greco, P. Nason. JHEP **05** (1998) 007.

[11] B. A. Kniehl, G. Kramer, I. Schienbein, and H. Spiesberger, Phys. Rev. Lett. **96**, 012011 (2006).

[12] B. A. Kniehl, and G. Kramer, Phys. Rev. D **74**, 037502 (2006).

[13] B. A. Kniehl, G. Kramer, I. Schienbein, and H. Spiesberger, Eur. Phys. J. C **41**, 2082 (2012).

[14] V. N. Gribov and L. N. Lipatov, Sov. J. Nucl. Phys. **15**, 438 (1972) [Yad. Fiz. **15**, 781 (1972)]; Yu. L. Dokshitzer, Sov. Phys. JETP **46**, 641 (1977) [Zh. Eksp. Teor. Fiz. **73**, 1216 (1977)]; G. Altarelli and G. Parisi, Nucl. Phys. **B126**, 298 (1977).

[15] OPAL Collaboration, K.Ackerstaff *et al.*, Eur. Phys. J. C **1**, 439 (1998); OPAL Collaboration, G. Alexander *et al.*, Z. Phys. C **72**, 1 (1996).

[16] M. Cacciari, and P. Nason. JHEP **09** (2003) 006.

[17] M. Cacciari, S. Frixione, N. Houdeau, M. L. Mangano, P. Nason, and G. Ridolfi JHEP **1210**, 137 (2012).

[18] R. Maciula, M. Luszczak, A. Szczurek, EPJ Web of Conferences **37**, 06008 (2012).

[19] Ph. Hagler, R. Kirschner, A. Schafer, L. Szymanowski, and O. V. Teryaev, Phys. Rev. D **62**, 071502(R) (2000).

[20] B. A. Kniehl, V. A. Saleev, A. V. Shipilova, E. V. Yatsenko, Phys. Rev. **D84** , 074017 (2011).

[21] M. A. Nefedov, V. A. Saleev, A. V. Shipilova Phys. Rev. D. **D87** , 094030 (2013).

[22] V. A. Saleev, Phys. Rev. D **78**, 034033 (2008).

[23] V. A. Saleev, Phys. Rev. D. **78**, 114031 (2008).

[24] B. A. Kniehl, M. A. Nefedov, V. A. Saleev, Phys. Rev. D. **89**, 114016 (2014).

[25] M. A. Nefedov, N. N. Nikolaev, V. A. Saleev Phys. Rev. D. **87**, 014022 (2013).

[26] B. A. Kniehl, A. V. Shipilova, and V. A. Saleev, Phys. Rev. D **81**, 094010 (2010).

[27] V. A. Saleev, A. V. Shipilova Phys. Rev. D. **86**, 034032 (2012).

[28] B. A. Kniehl, V. A. Saleev, and D. V. Vasin, Phys. Rev. D **73**, 074022 (2006).

[29] B. A. Kniehl, V. A. Saleev, and D. V. Vasin, Phys. Rev. D **74**, 014024 (2006).

[30] V. A. Saleev and D. V. Vasin, Phys. Rev. D **68**, 114013 (2003); Phys. Atom. Nucl. **68**, 94 (2005) [Yad. Fiz. **68**, 95 (2005)].

[31] V. A. Saleev, M. A. Nefedov, A. V. Shipilova, Phys. Rev. D**85**, 074013 (2012).

[32] M. A. Nefedov, V. A. Saleev, A. V. Shipilova, Phys. Rev. D**88**, 014003 (2013).

[33] E. A. Kuraev, L. N. Lipatov, and V. S. Fadin, Sov. Phys. JETP **44**, 443 (1976) [Zh. Eksp. Teor. Fiz. **71**, 840 (1976)]; I. I. Balitsky and L. N. Lipatov, Sov. J. Nucl. Phys. **28**, 822 (1978) [Yad. Fiz. **28**, 1597 (1978)].

[34] E. A. Kuraev, L. N. Lipatov, V. S. Fadin, Phys. Lett. B**60**, 50 (1975).

[35] V. S. Fadin, R. Fiore, Phys. Rev. D**64** 114012, (2001) .

[36] L. N. Lipatov, Nucl. Phys. **B452**, 369 (1995).

[37] L. N. Lipatov and M. I. Vyazovsky, Nucl. Phys. **B597**, 399 (2001).

[38] E. N. Antonov, L. N. Lipatov, E. A. Kuraev, and I. O. Cherednikov, Nucl. Phys. **B721**, 111 (2005).

[39] A. van Hameren, K. Kutak, and T. Salwa, Phys. Lett. **B727**, 226 (2013); A. van Hameren, P. Katko, and K. Kutak, JHEP **1301**, 078 (2013).

[40] M. A. Kimber, A. D. Martin, and M. G. Ryskin, Phys. Rev. D **63**, 114027 (2001).

[41] M. Ciafaloni, Nucl. Phys. **B296**, 49 (1988); S. Catani, F. Fiorani, G. Marchesini, Phys. Lett **B234** 339, (1990); Nucl. Phys. **B336** 18, (1990).

[42] CDF Collaboration, F. Abe *et al.*, Phys. Rev. Lett. **79**, 572 (1997); **79**, 578 (1997); CDF Col-

laboration, T. Affolder *et al.*, Phys. Rev. Lett. **85**, 2886 (2000); CDF Collaboration, D. Acosta *et al.*, Phys. Rev. D **71**, 032001 (2005); CDF Collaboration, F. Abe *et al.*, Phys. Rev. Lett. **75**, 4358 (1995); CDF Collaboration, D. Acosta *et al.*, *ibid.* **88**, 161802 (2002); CDF Collaboration, V. M. Abazov *et al.*, Phys. Rev. Lett. **94**, 232001 (2005).

[43] ATLAS Collaboration, G. Aad et al. Phys. Rev. D **87**, 052004 (2013); CMS Collaboration, S. Chatrchyan et al. Phys. Rev. D **83**, 112004 (2011); LHCb Collaboration, R. Aaij et al. Eur. Phys. J. **C72**, 2025 (2012).

[44] B. Mele, P. Nason, Nucl. Phys. **B361**, 626 (1991).

[45] V. S. Fadin and L. N. Lipatov, Nucl. Phys. **B477**, 767 (1996).

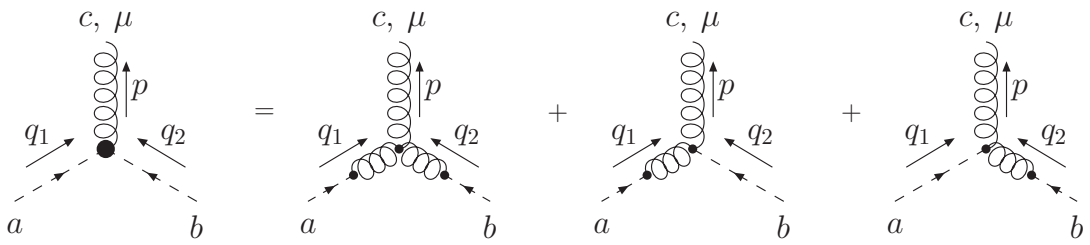

FIG. 1: Feynman diagrams for the subprocess (2).

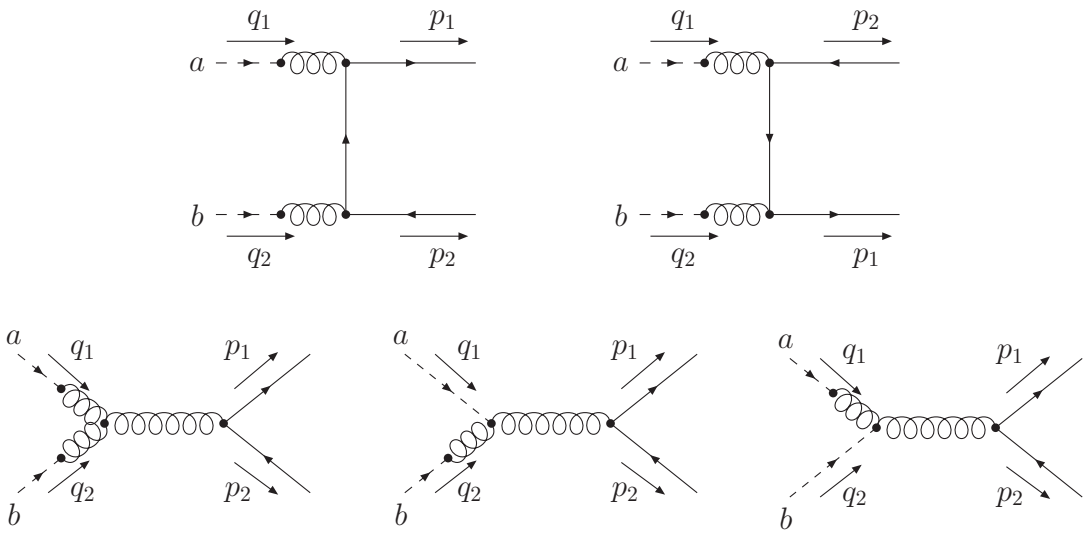

FIG. 2: Feynman diagrams for the subprocess (3).

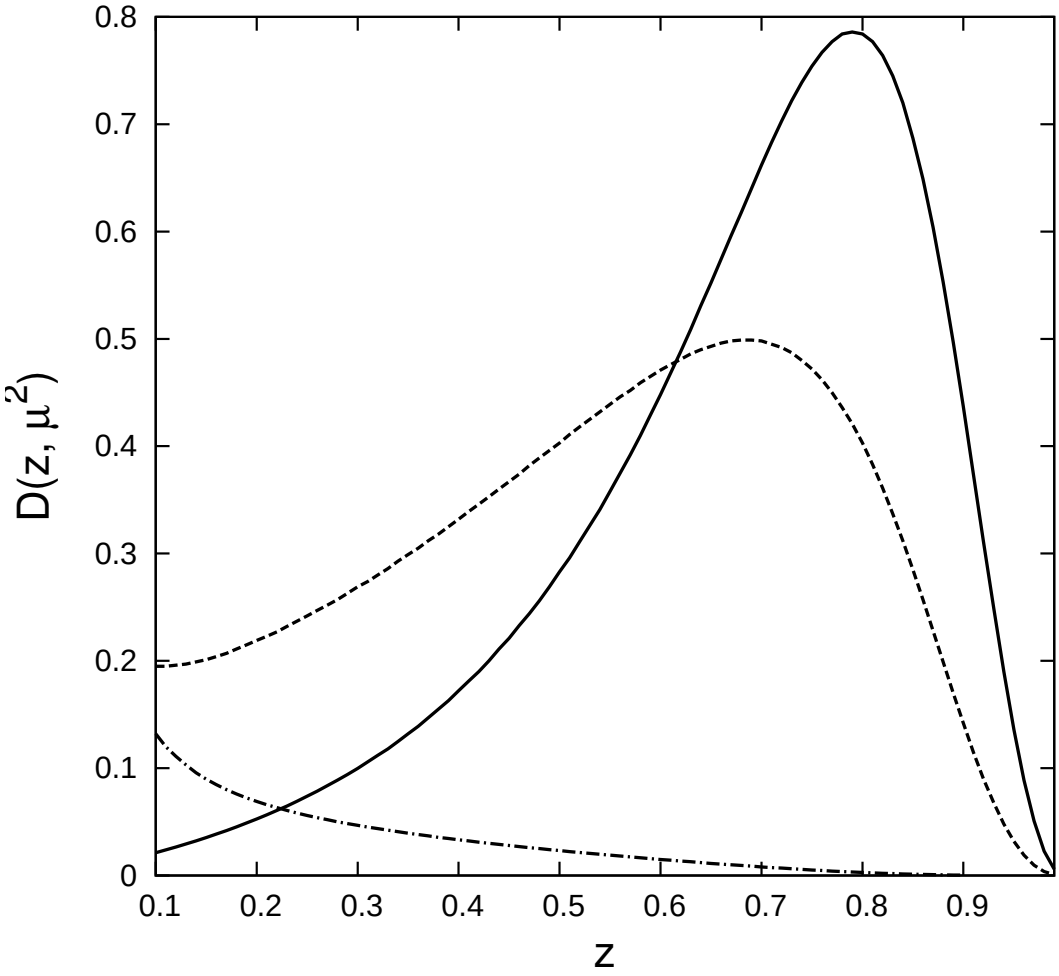

FIG. 3: The fragmentation function $D(z, \mu^2)$ of c-quarks and gluons into $D^\star$ mesons from Ref. [12] at the $\mu^2 = \mu_0^2 = 2.25$ GeV^2 (solid curve for c-quark, the fragmentation function of gluon is negligible) and $\mu^2 = 100$ GeV^2 (dashed line for c-quark, dash-dotted for gluon).

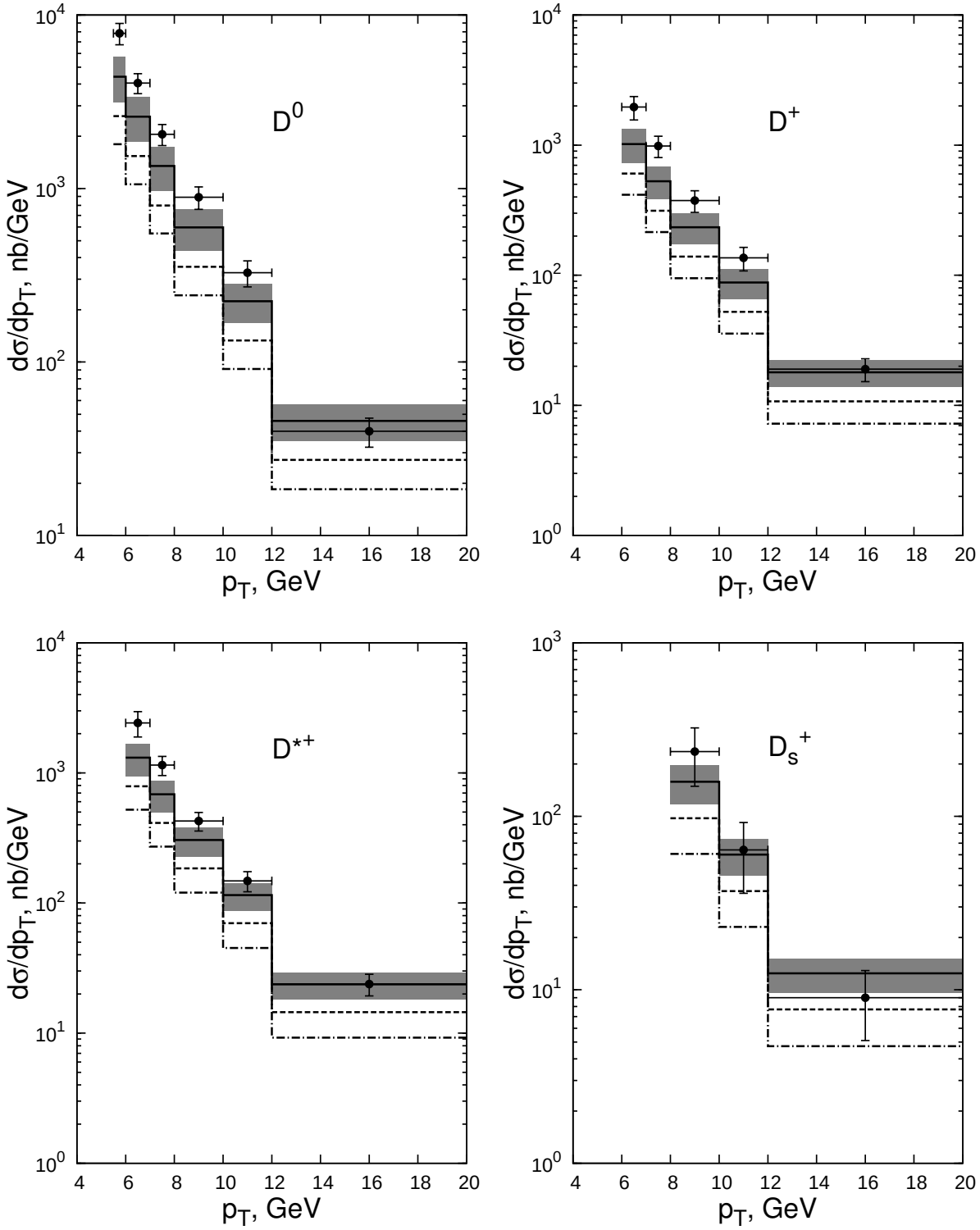

FIG. 4: Transverse momentum distributions of D^0 (left, top), D^+ (right, top), $D^{\star+}$ (left, bottom), and D_s^+ (right, bottom) mesons in $p\bar{p}$ scattering with $\sqrt{S} = 1.96$ TeV and $|y| < 1.0$. Dashed line represents the contribution of gluon fragmentation, dash-dotted line – the c-quark-fragmentation contribution, solid line is their sum. The CDF data at Tevatron are from the Ref. [7].

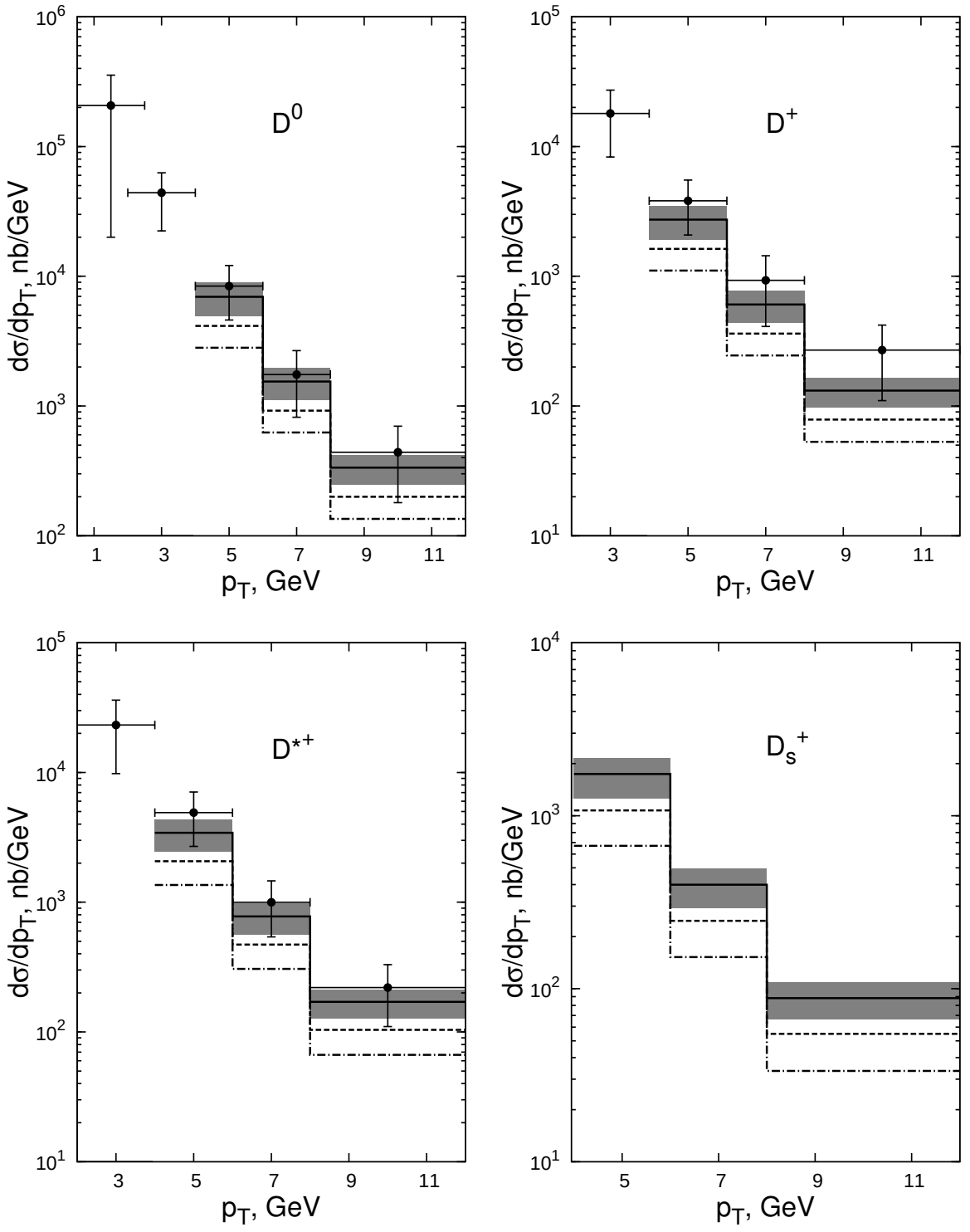

FIG. 5: Transverse momentum distributions of D^0 (left, top), D^+ (right, top), $D^{\star+}$ (left, bottom), and D_s^+ (right, bottom) mesons in pp scattering with $\sqrt{S} = 2.76$ TeV and $|y| < 0.5$. The notations as in the Fig. 4. The ALICE data at LHC are from the Ref. [4].

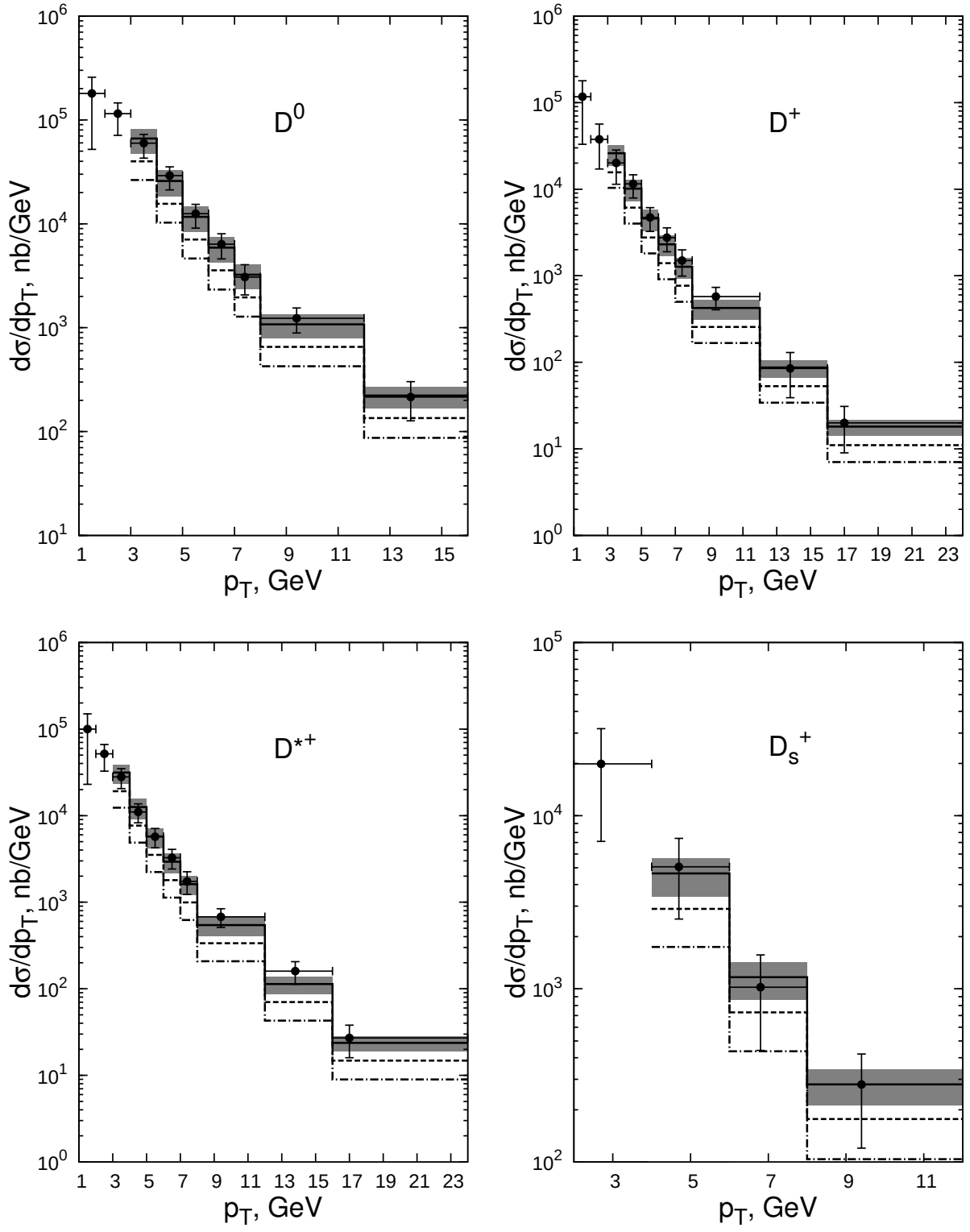

FIG. 6: Transverse momentum distributions of D^0 (left, top), D^+ (right, top), $D^{\star+}$ (left, bottom), and D_s^+ (right, bottom) mesons in pp scattering with $\sqrt{S} = 7$ TeV and $|y| < 0.5$. The notations as in the Fig. 4. The ALICE data at LHC are from the Ref. [5]. .

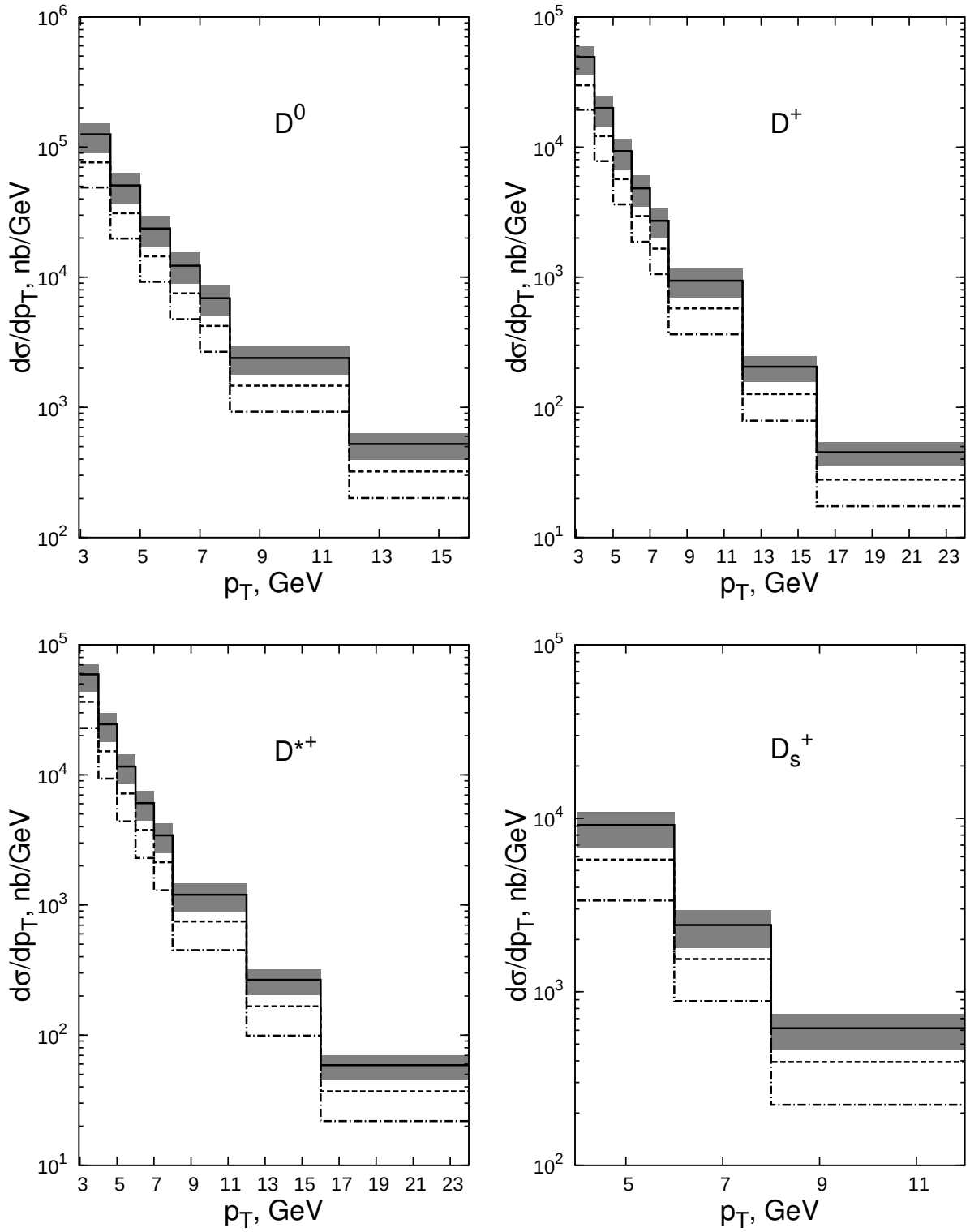

FIG. 7: Theoretical predictions for the transverse momentum distributions of D^0 (left, top), D^+ (right, top), $D^{\star +}$ (left, bottom), and D_s^+ (right, bottom) mesons in pp scattering at $\sqrt{S} = 14$ TeV and $|y| < 0.5$ obtained in the LO PRA. The notations as in the Fig. 4.

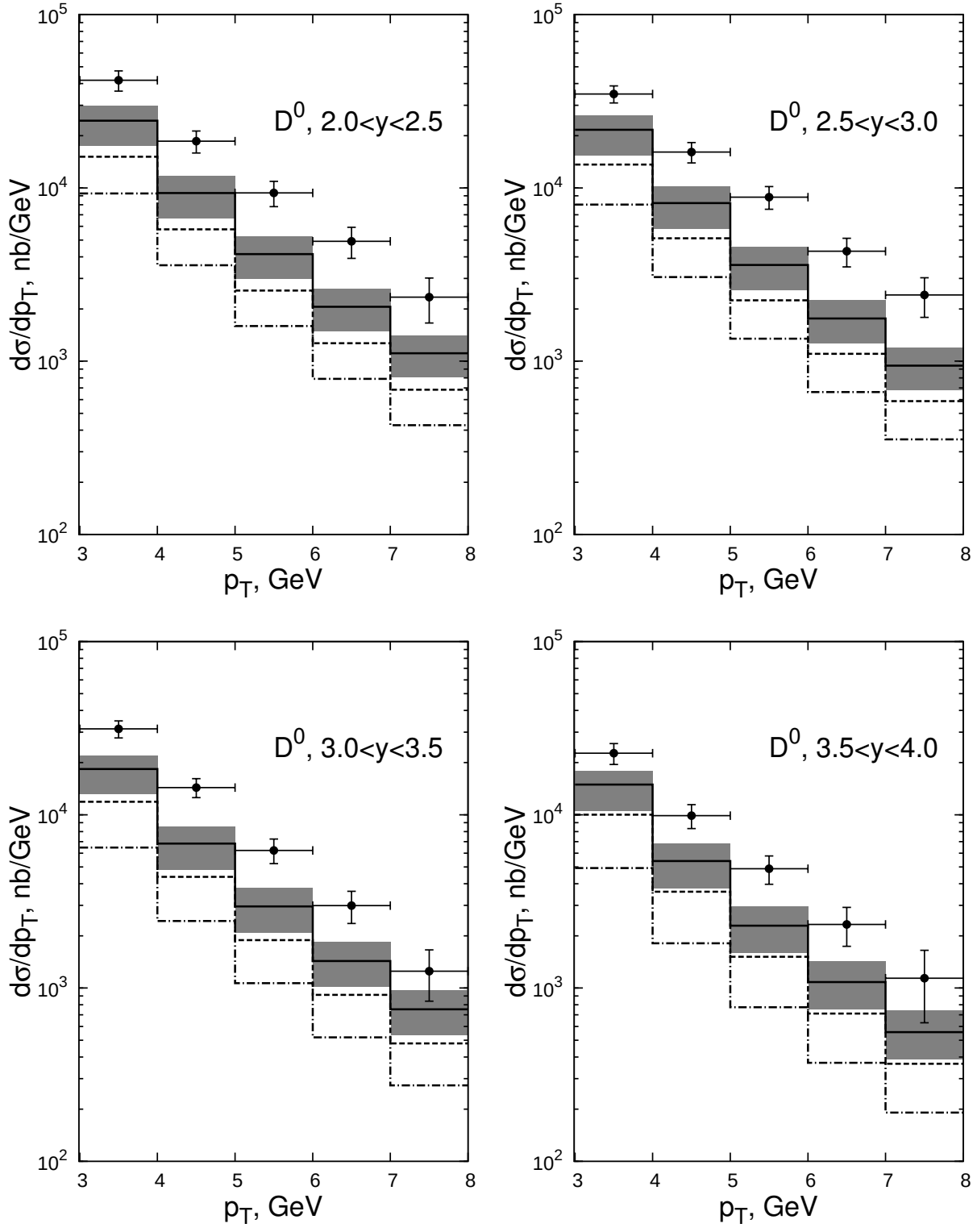

FIG. 8: Transverse momentum distributions of D^0 mesons in forward rapidity region in pp scattering with $\sqrt{S} = 7$ TeV. The LHCb data at LHC are from the Ref. [8]. The notations as in the Fig. 4.

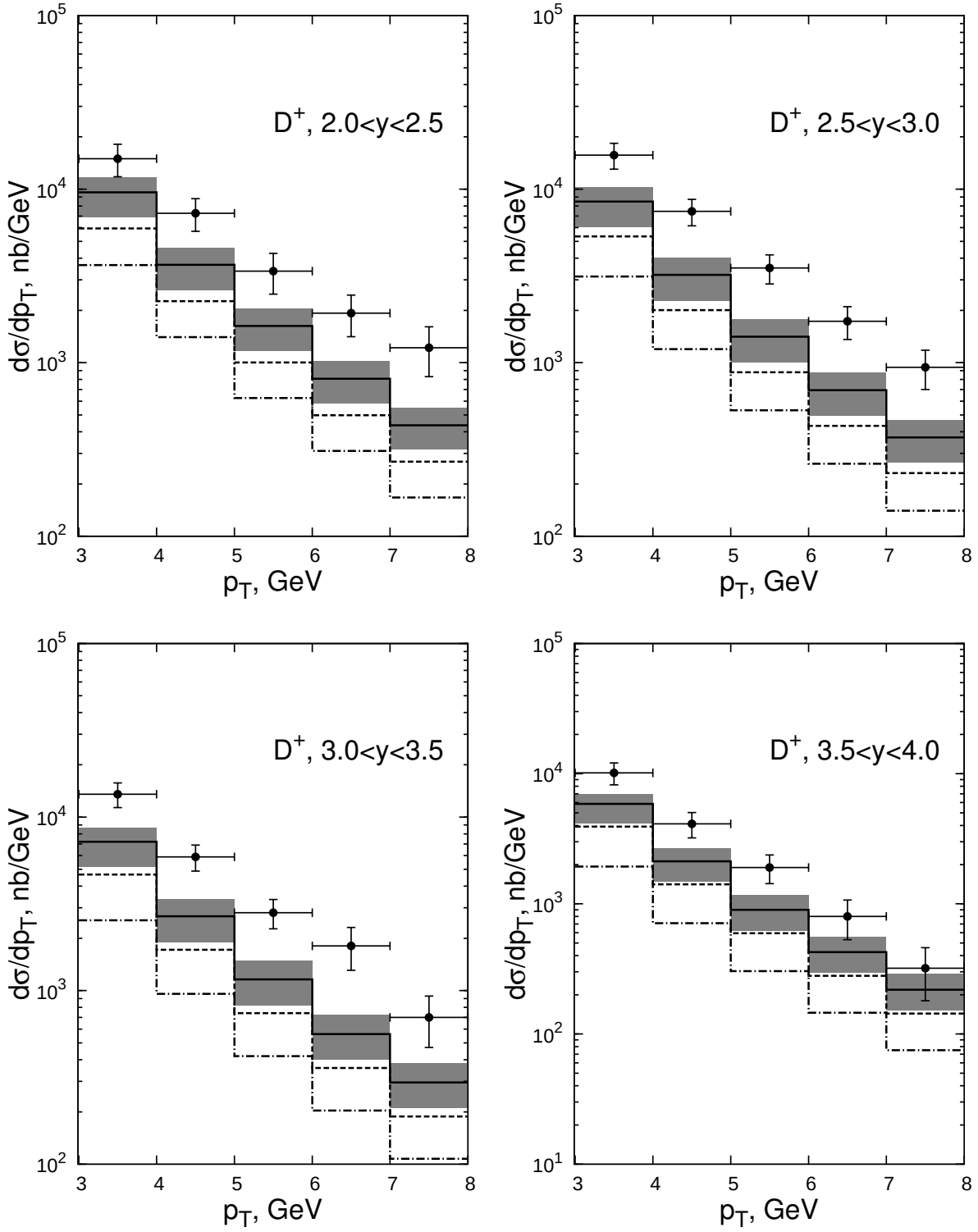

FIG. 9: The same as in the Fig. 8 for D^+ mesons

.

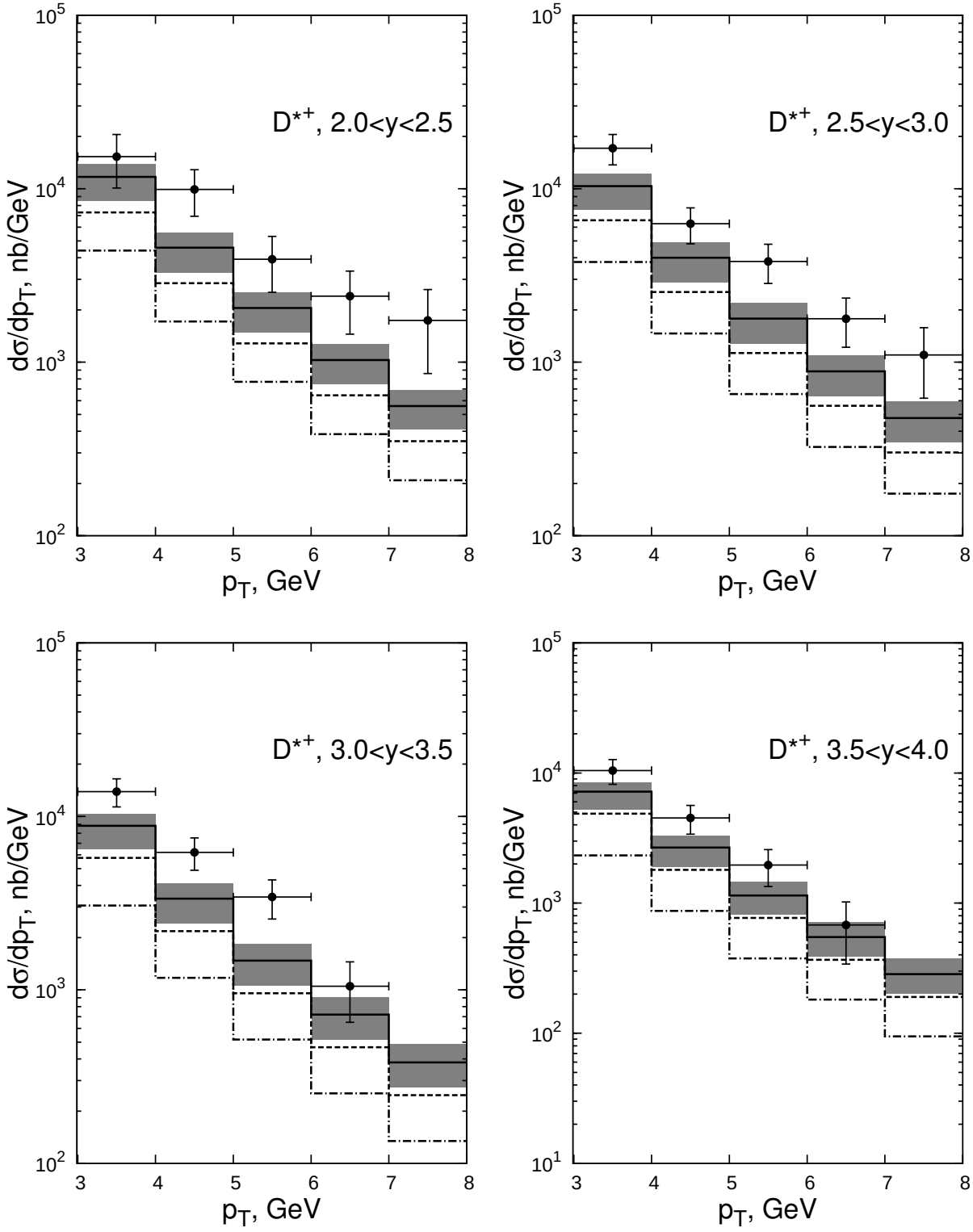

FIG. 10: The same as in the Fig. 8 for D^{*+} mesons.

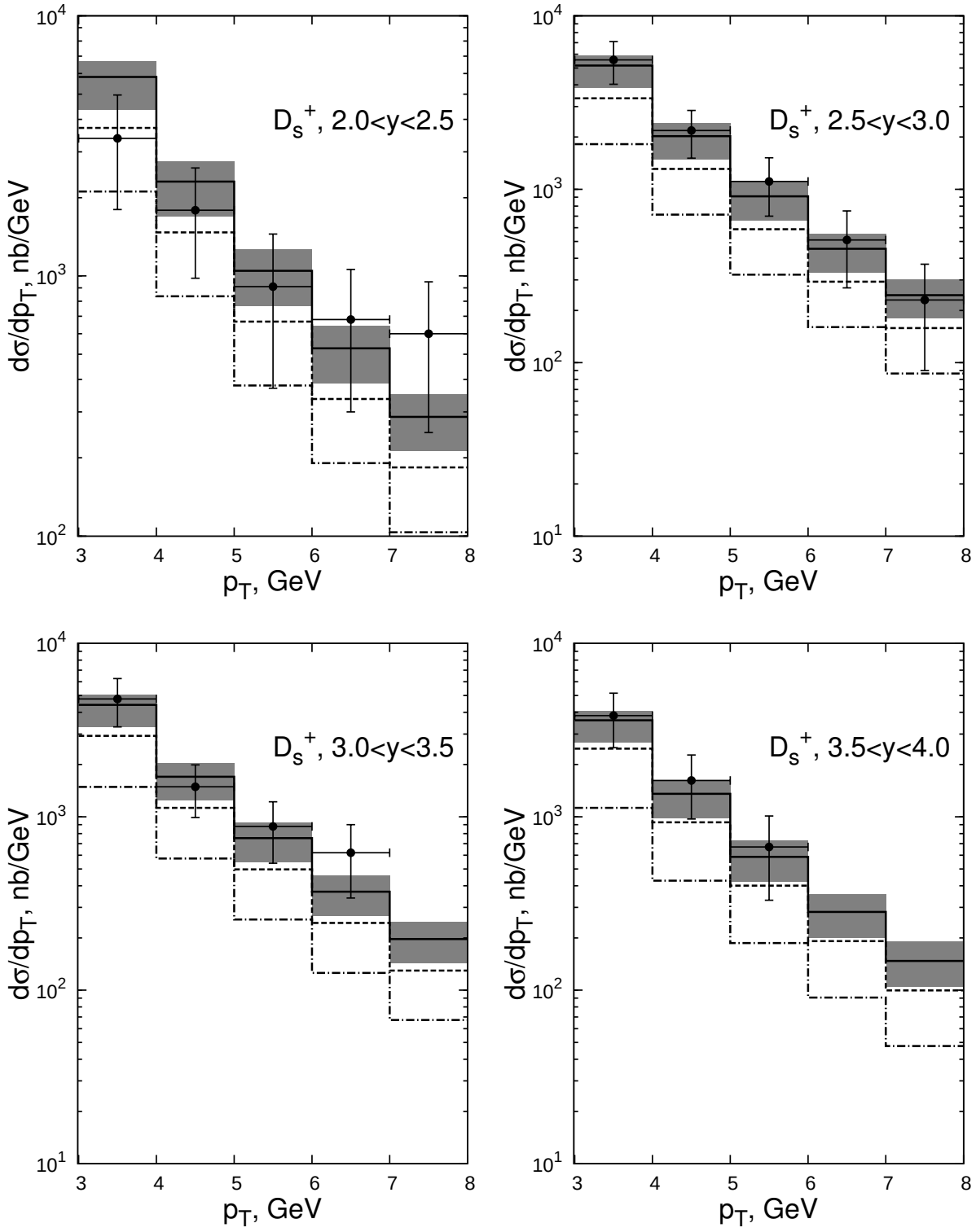

FIG. 11: The same as in the Fig. 8 for D_s^+ mesons.

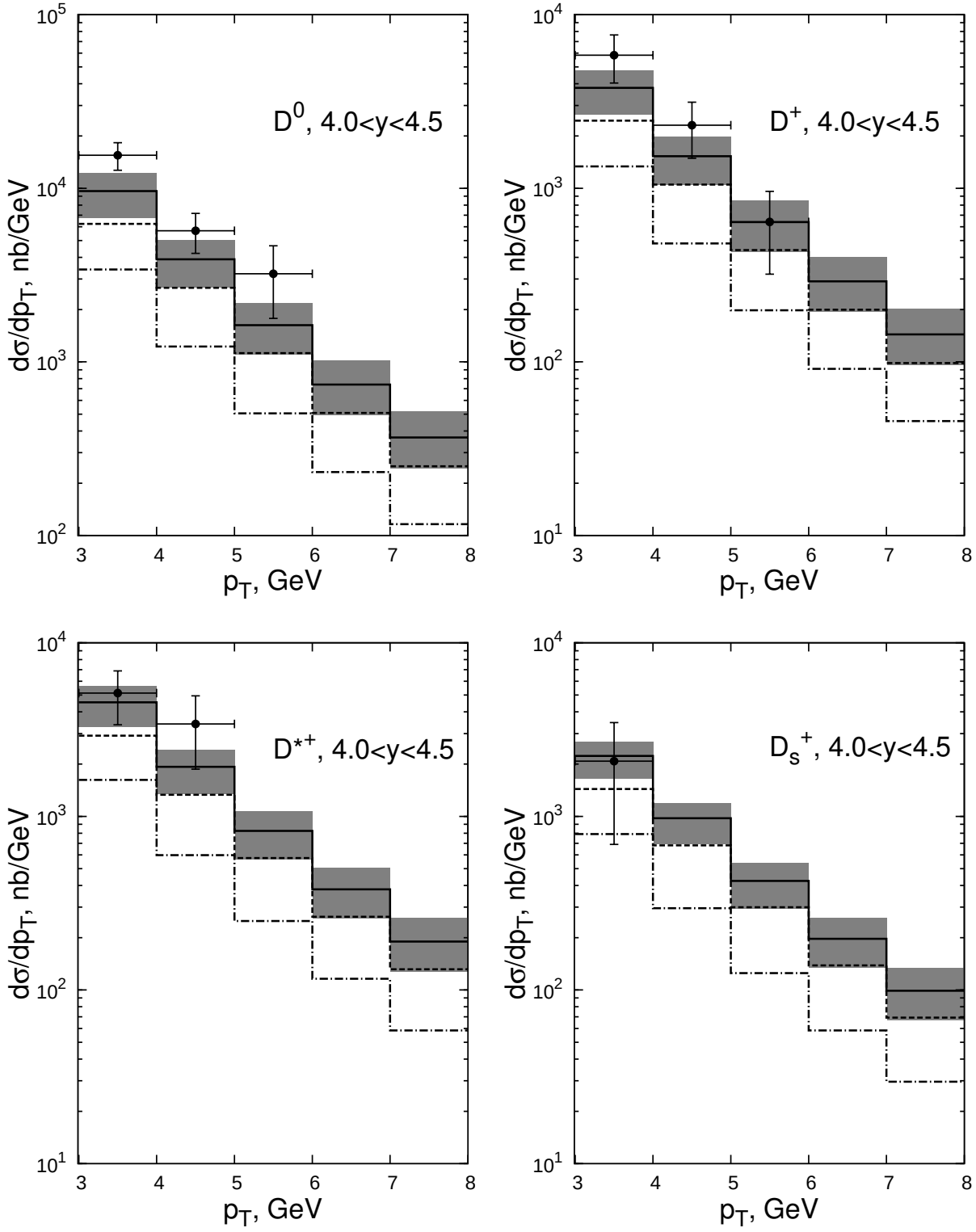

FIG. 12: Transverse momentum distributions of D^0 (left, top), D^+ (right, top), $D^{\star+}$ (left, bottom), and D_s^+ (right, bottom) mesons in forward rapidity region in pp scattering with $\sqrt{S} = 7$ TeV and $4.0 < y < 4.5$. The LHCb data at LHC are from the Ref. [8]. The notations as in the Fig. 4.